ornl

ORNL/ATD-36

OAK RIDGE NATIONAL LABORATORY

MARTIN MARIETTA

DESIGN AND PERFORMANCE OF AN AXIAL AIR-GAP SOLUTION PUMP MOTOR

R. A. Hawsey
C. W. Sohns
D. S. Daniel
J. M. Bailey

May 1990

OPERATED BY
MARTIN MARIETTA ENERGY SYSTEMS, INC.
FOR THE UNITED STATES
DEPARTMENT OF ENERGY

ORNL/ATD--36

DE91 009988

DESIGN AND PERFORMANCE OF AN AXIAL AIR-GAP SOLUTION PUMP MOTOR

R. A. Hawsey

Applied Technology Division

C. W. Sohns

Instrumentation and Controls Division

D. S. Daniel

Applied Technology Division

J. M. Bailey

The University of Tennessee

Date Published—May 1990

Prepared by the
Oak Ridge National Laboratory
Oak Ridge, Tennessee 37831-7294
operated by
MARTIN MARIETTA ENERGY SYSTEMS, INC.
for the
U.S. DEPARTMENT OF ENERGY
under contract DE-AC05-84OR21400

TABLE OF CONTENTS

LIST OF FIGURES

LIST OF TABLES

EXECUTIVE SUMMARY

An axial air gap, permanent magnet, brushless dc motor has been designed and has been evaluated on a dynamometer to measure operating characteristics. The motor must deliver 0.167 hp (~120 W) to the pump rotor at 1800 rpm. Initial performance data with a half-bridge, Hall-probe synchronized drive system and a dry motor bearing did not achieve the desired motor performance. Subsequently, a commercial full-bridge, speed-regulated "sensorless" drive system was used to test the motor. The motor was operated successfully with a new, water-lubricated bearing system. The motor delivered the required 90 oz-in. of torque at 1800 rpm. These data revealed the need for rewinding the stator core to improve motor efficiency.

A second stator core, with deeper slots and additional turns of wire, was subsequently fabricated and tested. At 1800 rpm, the drive system could produce only 60 oz-in. of torque due to an unexpectedly high generated voltage. Motor efficiency was 60 to 70% at this torque level when the data were corrected for bearing and coupling drag.

MOTOR DESIGN

The permanent magnet motor consists of a tape-wound stator, slotted and wired, driving a six-pole ferrite-ring magnet attached to the solution pump rotor. The stator core, for these prototype tests, was wound with 0.005-in. MAGNESIL-N™ silicon steel tape. The tape was epoxy-dipped as it was wound to provide an insulating layer between each layer of tape to minimize magnetic losses. The slots were saw cut after winding the tape, and the copper wire coils were hand formed and inserted into the stator core. A potting compound will hold the coils in place for the final application. Figure 1 is a drawing of a typical stator core and a wiring description. The first stator tested was one-half as long axially as that shown in Fig. 1 and contained approximately one-half the wire turns.

DESCRIPTION OF THE DRIVE SYSTEMS

HALF-BRIDGE ADJUSTABLE-SPEED DRIVE

The half-bridge drive system built in-house for motor testing consists of only an inverter. The input power is variable voltage dc, which allows for speed control. Three stator-mounted Hall probes are used to sense the rotor position and control the phasing of the output transistors in the inverter. A schematic of the drive is shown in Fig. 2. The PC-board layout diagram is shown in Fig. 3. Table 1 is a bill of materials for the drive.

The inverter is a half-bridge configuration that has the capability of pulling current out of a motor phase lead. The motor neutral lead is connected to a positive current source. Current flow through the motor is always the same direction in the neutral lead and out of the appropriate phase lead. The approach does not use all the magnetic capabilities of the motor, but the drive electronics are much simpler than the conventional "push-pull" system.

G. E. DRIVE SYSTEM

The G. E. drive system is a sensorless, pulse-width modulated design with a "push-pull" output stage. The first system used (with the first stator) is large enough to drive a 5-hp motor; however, driving a small motor did not cause any difficulty. The sensorless feature replaces Hall probes by measuring generated voltage during a phase "off" time and thereby getting an indication of rotor position. This technique saves the cost of Hall probes and additional signal wires between the drive package and the motor. The push-pull output stage made full use of the motor magnetics and did not require a connection to be made to the neutral lead of the motor. The speed of the machine is selected by a command signal pulse width and is controlled by pulse width modulating the output transistors. This allows for good speed regulation without the use of a switching regulator.

Table 1. Bill of materials for half-bridge drive system

Item	Quantity	Reference	Part
1	1	C1	0.1 μF, 1 kV
2	1	C2	540 μF, 450 Vdc
3	3	D1, D2, D3	RWB100
4	2	J1, J3	Banana jack, red
5	2	J2, J4	Banana jack, black
6	3	Q1, Q2, Q3	2N3906
7	3	Q4, Q5, Q6	MJ10023
8	3	R1, R7, R13	510 Ω
9	3	R2, R8, R14	100 Ω
10	3	R3, R9, R15	160 kΩ
11	3	R4, R10, R16	650 Ω
12	3	R5, R11, R17	2.7 kΩ
13	3	R6, R12, R18	150 Ω
14	1	R19	30 Ω, 2 W
15	1	R20	500 Ω, 10 W
16	3	R21, R22, R23	1.6 kΩ, 2 W
17	1	U1	LM339
18	1	U5	LM7806

RESULTS

FIRST STATOR TESTS

Three sets of performance data have been taken on the original solution pump motor. The first set was taken with a dry rotor bearing and the half-bridge, Hall-probe synchronized drive system. Air gaps from 0.050 to 0.350 in. were tested at 0.050-in. increments. For each air-gap setting, a family of curves was produced to characterize motor torque vs speed for various drive voltages. These data are presented in Figs. 4 through 10. The voltages shown in these figures are dc voltages applied to the half-bridge inverter and directly correlate to the voltage applied to the motor.

The highest voltage used during these tests was 50 Vdc, which produced 18 oz-in. of torque at 1800 rpm when the air gap was set to 0.150 in. This is well below the required 90 oz-in. of torque because excessive motor heating limited the amount of voltage that could be applied during the tests. Motor overheating was addressed in a revised motor design where increased number of parallel turns were used in the motor winding.

Low motor torque was also caused in part by the losses in the dry thrust bearing that supported the rotor. The load on this bearing was a function of air-gap flux density, which varied with the size of the air gap. It follows that tests with 0.050-in. air gaps had the greatest bearing loss, and those tests performed with 0.350-in. air gaps had less bearing loss. The actual loss magnitude was not measured.

The dry-rotor bearing system was replaced with a water-soaked system that would be appropriate in the actual application of this solution pump. A second set of data was taken with this bearing system at air gaps of 0.050 to 0.350 in. in increments of 0.100 in. The data are shown in Figs. 11 through 14.

As with the first set of performance data, a family of curves was produced at each air gap by applying different voltages to the drive package and measuring speed as the load was changed. The voltage was again limited so the motor would not overheat. A maximum output torque of 41 oz-in. was observed when 60 Vdc was applied to the drive package while the gap was set to 0.150 in.

Figure 15 is a plot of air-gap flux as a function of air gap for the water-bearing rotor. As the air gap is reduced, air-gap flux rises and so does thrust-bearing drag, as discussed earlier. This increased loss will lower motor efficiency at low air gaps as shown in Fig. 16. Figure 16 also shows a general falling off of motor efficiency with large (0.350-in.) air gaps. This occurs as a result of increased power loss in the winding resistance—larger motor currents are required to compensate for the lower generated voltage. The graph clearly shows that motor efficiency is a peaked function and that 40% efficiency can be achieved with air gaps in the 0.150- to 0.250-in. range.

The third set of data with the first stator was recorded using the rotor with the water-soaked bearing and a 5-hp G. E. sensorless drive system. This drive system is a full-bridge, speed-regulated system that produced data in a different form from that of the previous

nonspeed-regulated drive system. The data from this test are tabulated in Table 2 for air gaps of 0.150, 0.250, and 0.350 in. The required 90 oz-in. of torque was demonstrated at air gaps of 0.150 and 0.250 in. at relatively poor efficiencies of 25 and 35%, respectively. As noted earlier, the motor efficiency was enhanced in the revised motor design (see the next section of this report) by increasing the number of parallel turns of conductor.

SECOND STATOR TESTS

The revised axial-gap pump motor was connected to a 1-hp G.E. sensorless drive system and tested on the dynamometer. Initial testing revealed an instability in the drive system speed control, which caused the motor to hunt around the desired operating speed. This problem was discussed with G.E. representatives, and they offered to modify the drive system with new software. The drive system was sent back to G.E., where the new software was installed. The original software used current control in the speed algorithm, while the new software uses voltage control.

The second effort to test the drive system and revised motor was more successful in that stable speed regulation was demonstrated. The air gap was first set to 0.250 in., and the motor speed was set to 18.9 Hz, where various shaft loads were applied. The data from this test are presented in Table 3. The efficiency numbers listed do not consider dynamometer shaft coupler loss or thrust bearing loss, which results in lower efficiencies.

The motor speed was then stepped up to 30 Hz or 1800 rpm, where it will normally be operated. As the shaft load was increased, data were recorded in Table 3 up to ~60 oz-in., where the sensorless drive system lost synchronization with the motor. This was probably a result of low air-gap flux being excessively perturbated by stator flux, thus upsetting the generated voltage from which the drive system was controlled. Smaller air gap or stronger magnets would reduce the effect.

For the next set of tests, the air gap was increased to 0.350 in., and the speed was maintained at 30 Hz or 1800 rpm. As before, the shaft torque was increased in steps until the drive system lost synchronization at or near 55-oz-in. The data for this test are presented in Table 3. The efficiency listed in the table does not consider the loss in the bearing or coupler, so it is quite conservative.

The final air gap was set to 0.150 in., and the speed was set to 30 Hz or 1800 rpm. An additional wattmeter was added between the drive system and the motor so that individual component efficiencies could be monitored along with phase-to-phase motor voltage and current. These data are shown in Table 4. During the test, motor speed fell out of regulation when shaft load was increased to 60 oz-in. This results when the maximum output voltage is required from the drive system to overcome the vector sum of the generated voltage and that voltage necessary to drive the required current through the resistive winding.

Table 2. Axial-gap pump motor performance data with 5-hp G. E. drive

T (oz-in.)	Speed (rpm)	P_{out} (W)	P_{in} (W)	I_{ϕ} (A)	V_{ϕ} (V)	Eff. (%)
0.150-in. air gap						
20	1808	26.74	58	0.84	44.5	46.1
40	1800	53.23	158	1.57	57.2	33.7
60	1796	79.68	260	2.04	66.4	30.6
90	1795	119.45	473	2.73	77.5	25.2
0.250-in. air gap						
20	1800	26.6				
40	1791	52.9	102	1.53	58.7	52
60	1786	79.2	250	1.96	71.4	32
90	1770	117.8	360	2.84	81.8	33
0.350-in. air gap						
20	1800	26.6	96	1.29	52.3	27.7
40	1800	53.23	191	1.86	63.4	27.8
60	1795	79.63	341	2.48	76.6	23.4

Table 3. Stator performance

Copper winding (°F)	Speed (rps)	T (oz-in.)	Drive input (W)	Shaft power (W)	Efficiency (%)
Second stator at ~1200 rpm with 1-hp G.E. drive and 0.0250-in. air gap					
89	18.9	0	20.1	0	0
89	18.8	10	39.8	8.35	21
95	19.0	20	61.3	16.9	27.6
109	18.9	30	98.5	25.2	25.6
133	18.9	40	165	33.5	20.3
160	14.7	80	261	52.2	20.0
Second stator at ~1800 rpm with 1-hp G.E. drive and 0.250-in. air gap					
92	30.8	0	23.3	0	0
93	30.9	10	46.2	13.7	29.7
96	30.7	20	72.6	27.3	37.5
102	30.7	30	108.6	40.9	37.6
114	30.7	40	138	54.5	39.5
129	26.4	59	170.1	69	40.6
Second stator at ~1800 rpm with 1-hp G.E. drive and 0.350-in. air gap					
98	30.9	0	18.4	0	0
99	30.5	10	49.5	13.5	27.4
105	30.8	20	98.6	27.3	27.7
121	30.7	30	118	40.8	34.6
131	29.5	52	155	68.1	43.9

A measurement of dynamic bearing and coupling drag was made, and the power loss at 1800 rpm was ~20 W. If this 20-W loss is added to shaft power delivered to the dynamometer, a more realistic motor efficiency can be calculated. The results of this calculation are presented in Table 5, where actual motor efficiency is seen to be as high as 86% at 20 oz-in. and falls off as torque demand increases. However, taking the data from Table 5 as a guide, the efficiency of this motor, while delivering 90 oz-in. torque to the load, is expected to be in the 60 to 70% range.

Temperature measurements were made on the copper winding of the stator during all tests and noted in the appropriate tables. These temperatures are typically increasing toward some final value; however, the actual terminal motor temperature could only be measured if the motor were potted as intended in the final design.

Table 4. Performance of second stator at ~1800 rpm with 1-hp G.E. Drive and 0.150-in. air gap

Speed (Hz)	T (oz-in.)	Input power (W)	Motor power (W)	Motor voltage (ϕ-ϕ V)	Motor current (ϕ A)	Shaft power (W)
30.9	0	23.7	17.5	148	0.098	0
30.9	20	64	55	190	0.272	27.4
30.7	40	113	104	206	0.447	54.5
28.3	60	147	142	205	0.583	75.4

Table 5. Data from Table 4 with motor efficiency adjusted for ~20-W bearing and coupling losses

T (oz-in.)	Motor input (W)	Shaft power (W)	Total motor power (W)	Motor efficiency (%)
20	55	27.4	47.4	86.2
40	104	54.5	74.5	71.6
60	142	75.4	95.4	67.2

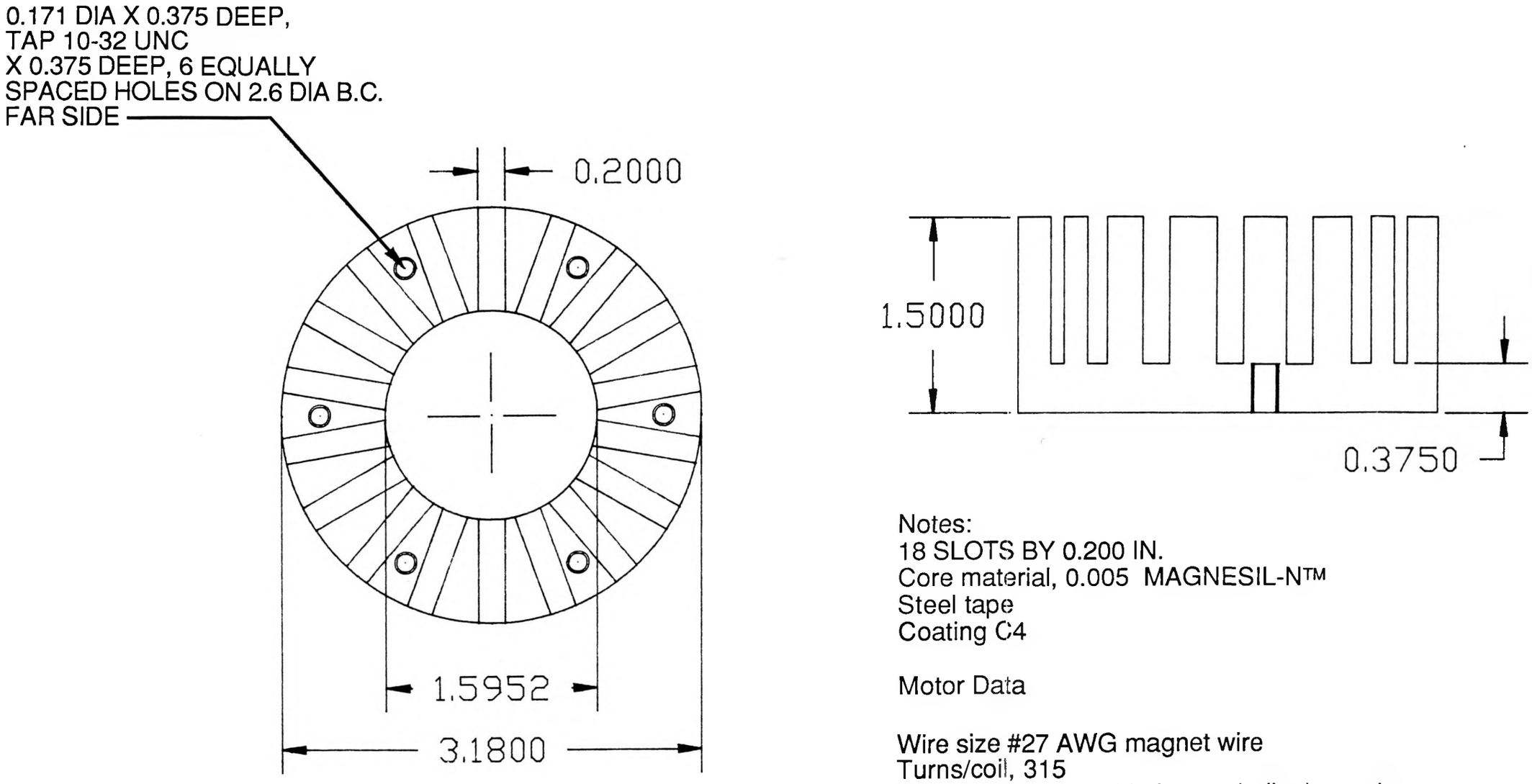

Notes:
18 SLOTS BY 0.200 IN.
Core material, 0.005 MAGNESIL-N™
Steel tape
Coating C4

Motor Data

Wire size #27 AWG magnet wire
Turns/coil, 315
Two coil sides (double layer winding) per slot
Span, 1-4
18 slots
1 slot/pole/phase
STAR connection

Fig. 1. Drawing of stator core with wiring description.

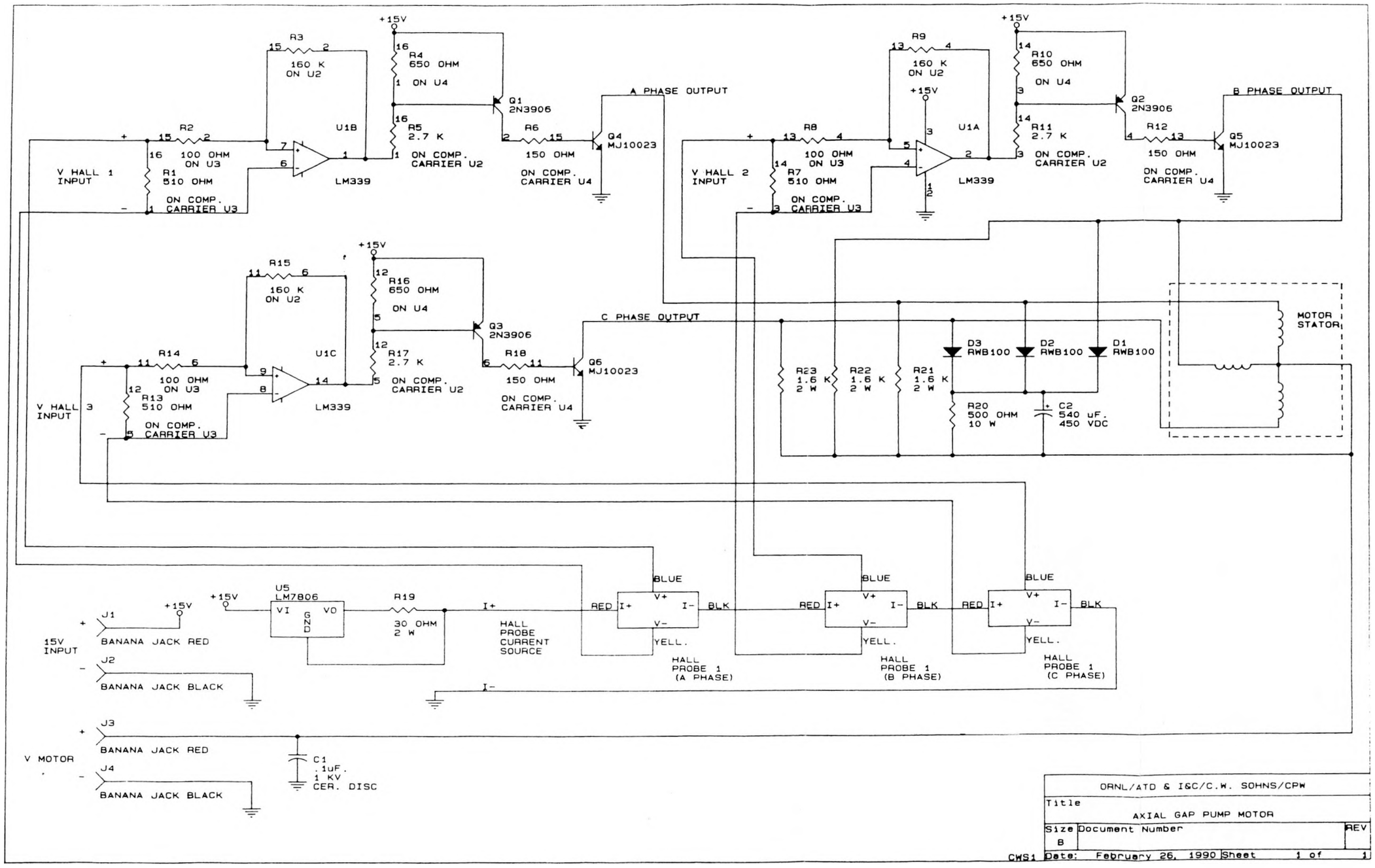

Fig. 2. Half-bridge drive for axial-gap pump motor.

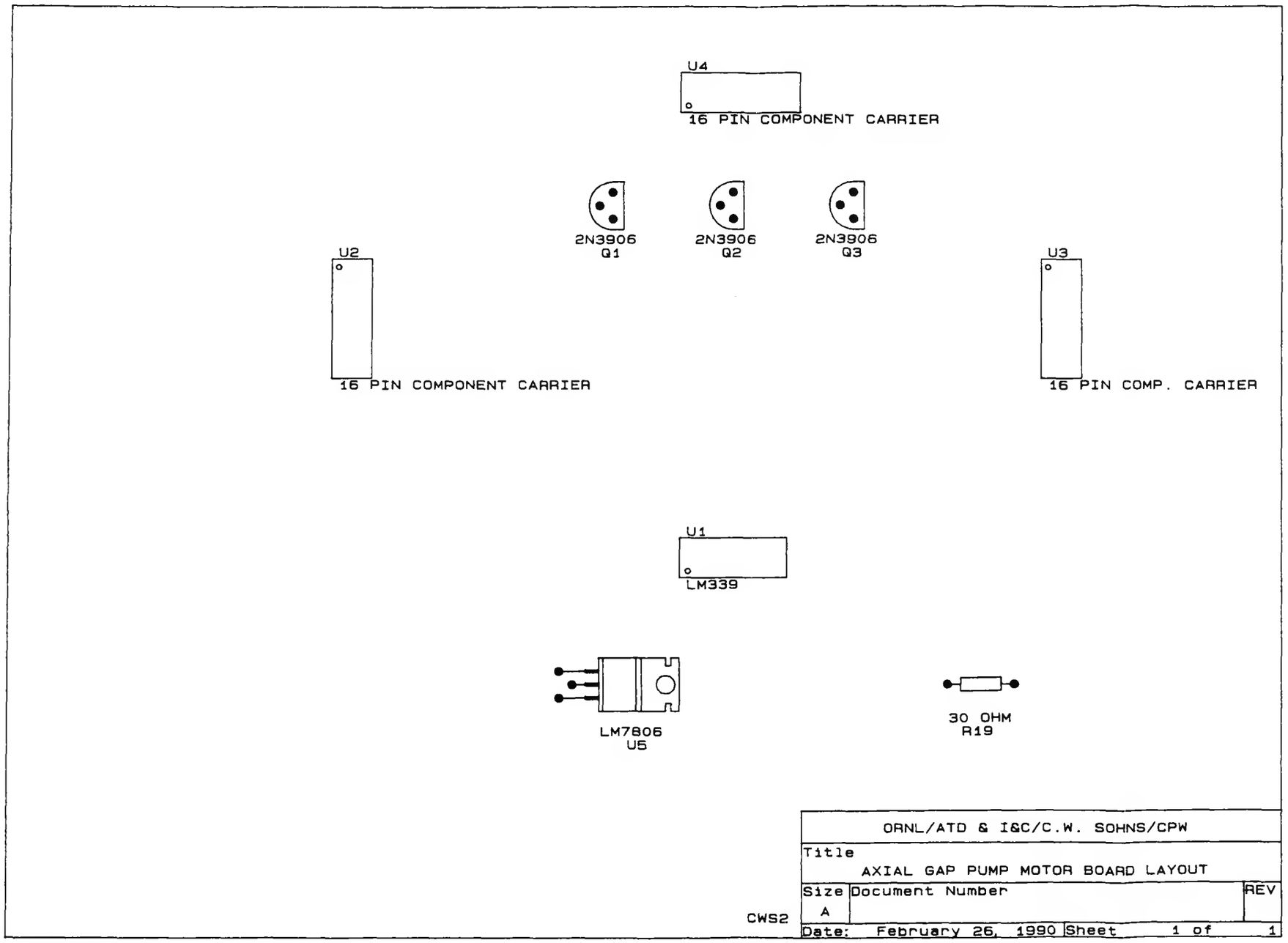

Fig. 3. Axial gap pump motor board layout.

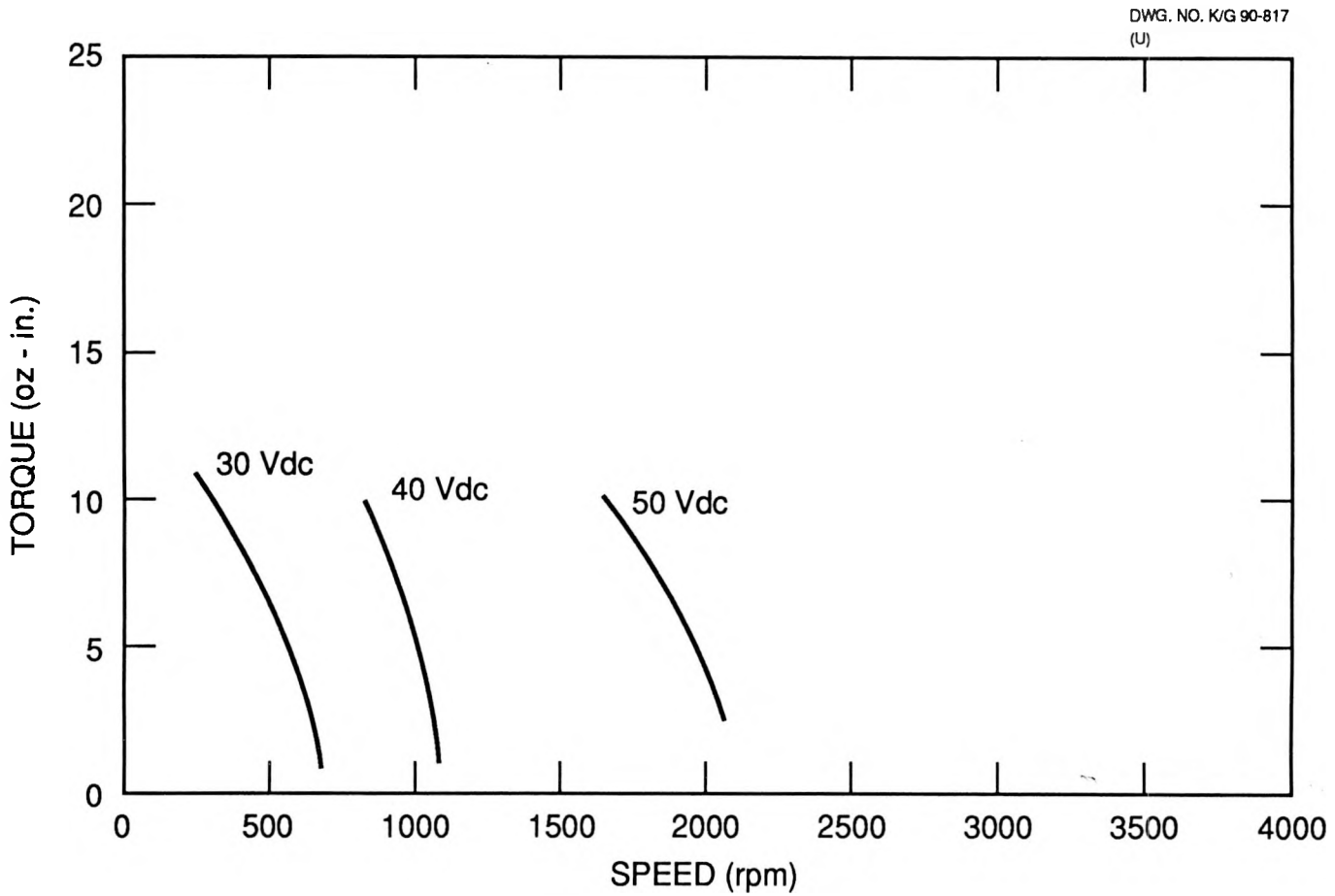

Fig. 4. Torque vs speed for 0.050-in. air gap and dry bearing using half-bridge drive system.

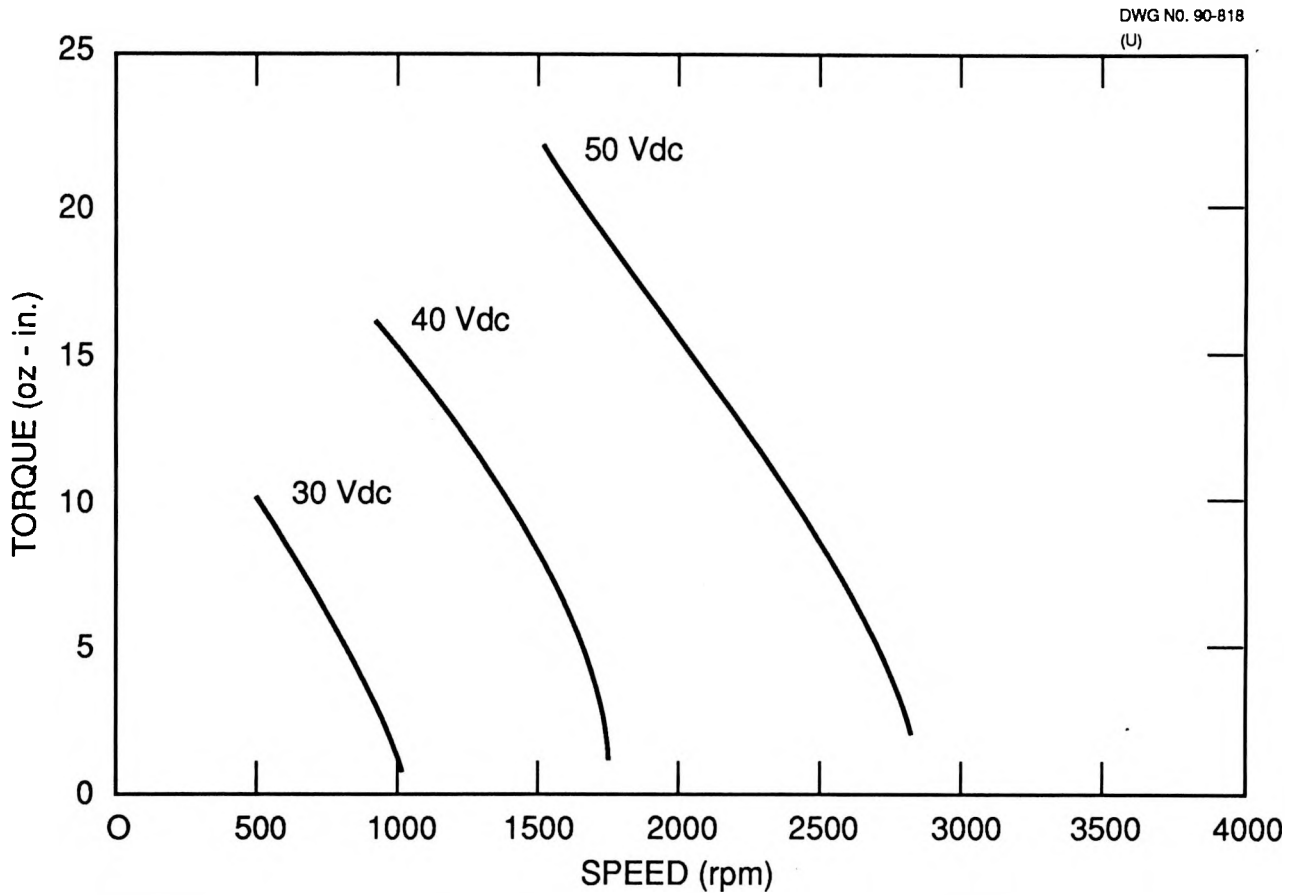

Fig. 5. Torque vs speed for 0.100-in. air gap and dry bearing using half-bridge drive system.

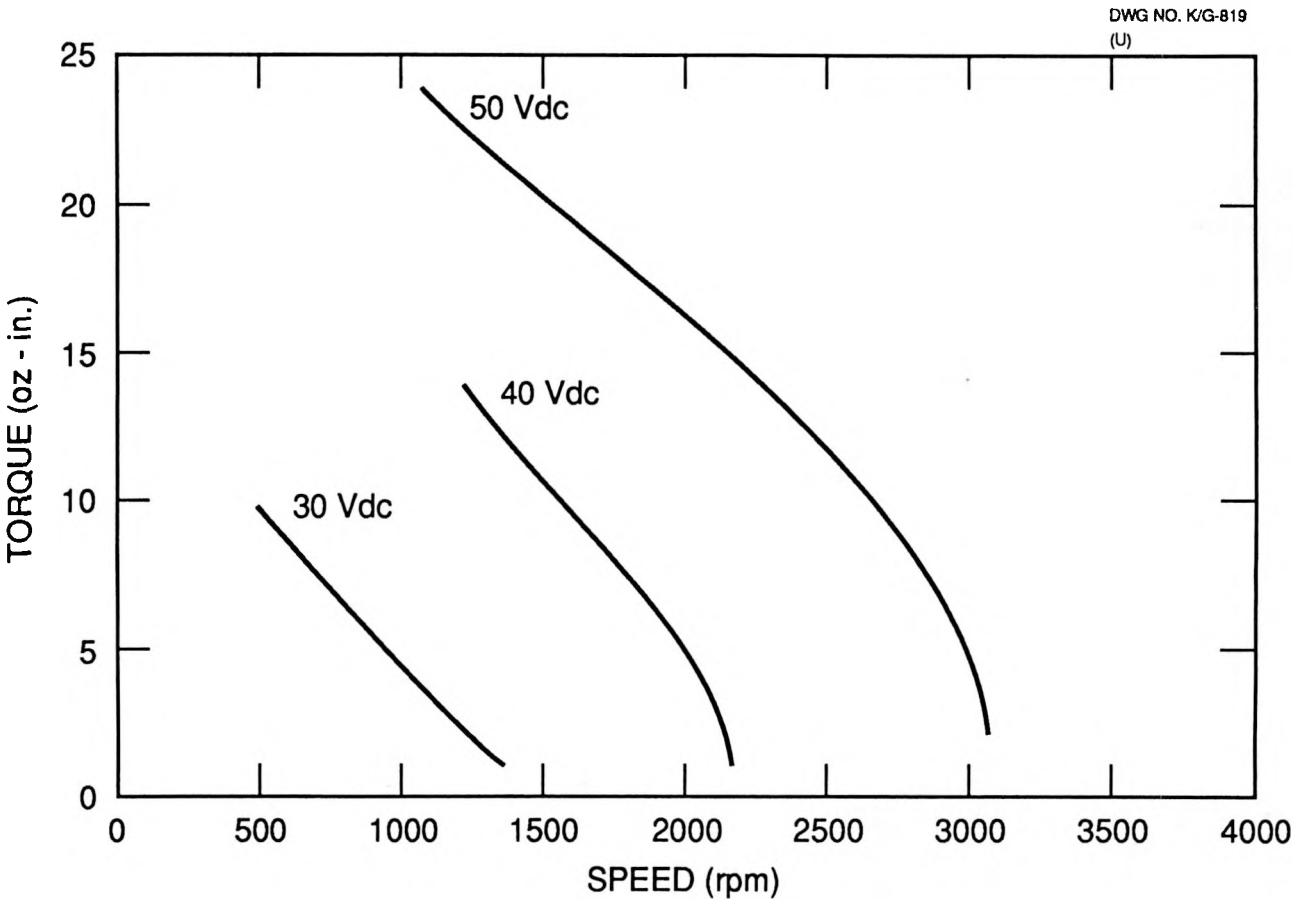

Fig. 6. Torque vs speed for 0.150-in. air gap and dry bearing using half-bridge drive system.

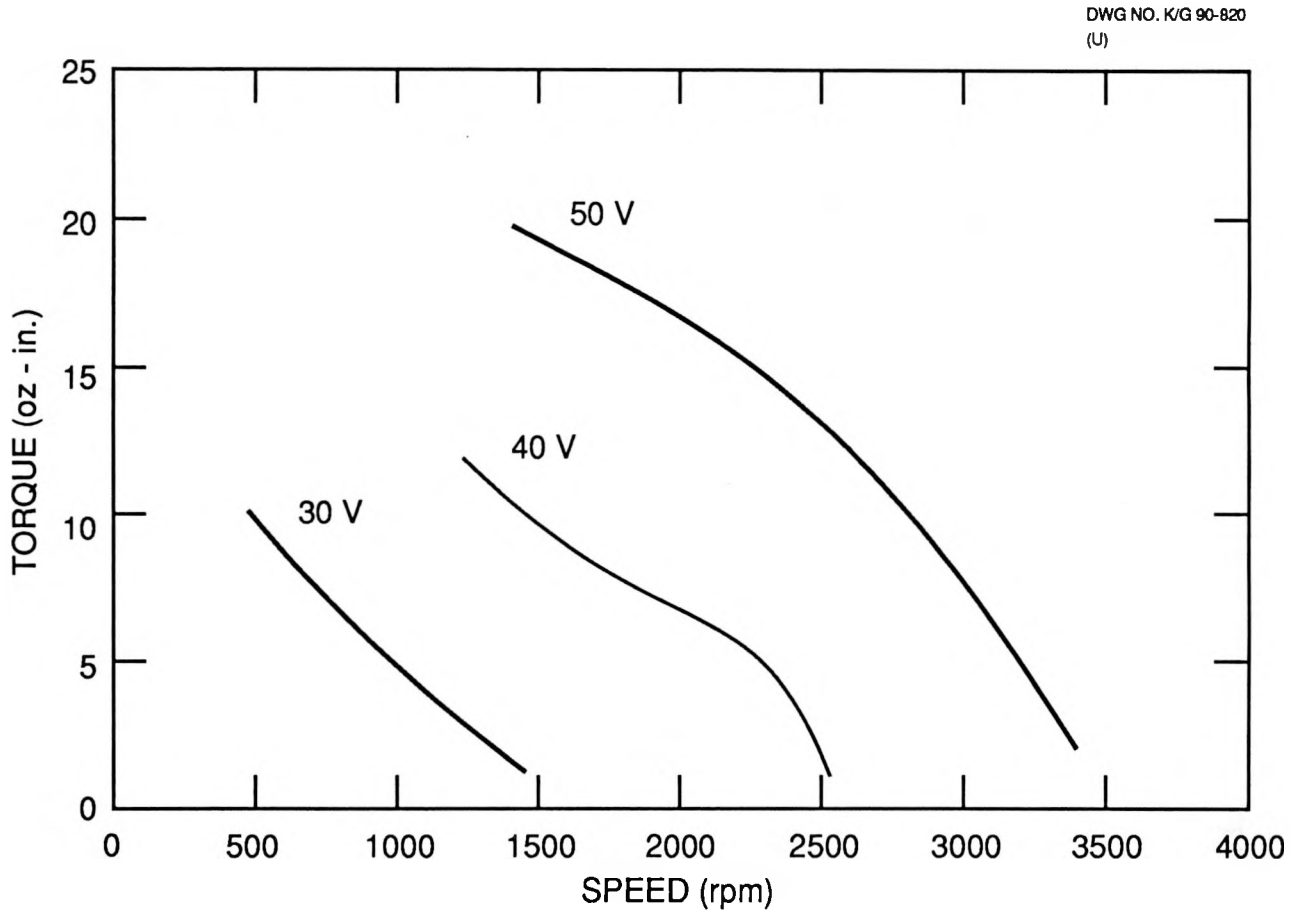

Fig. 7. Torque vs speed for 0.200-in. air gap and dry bearing using half-bridge drive system.

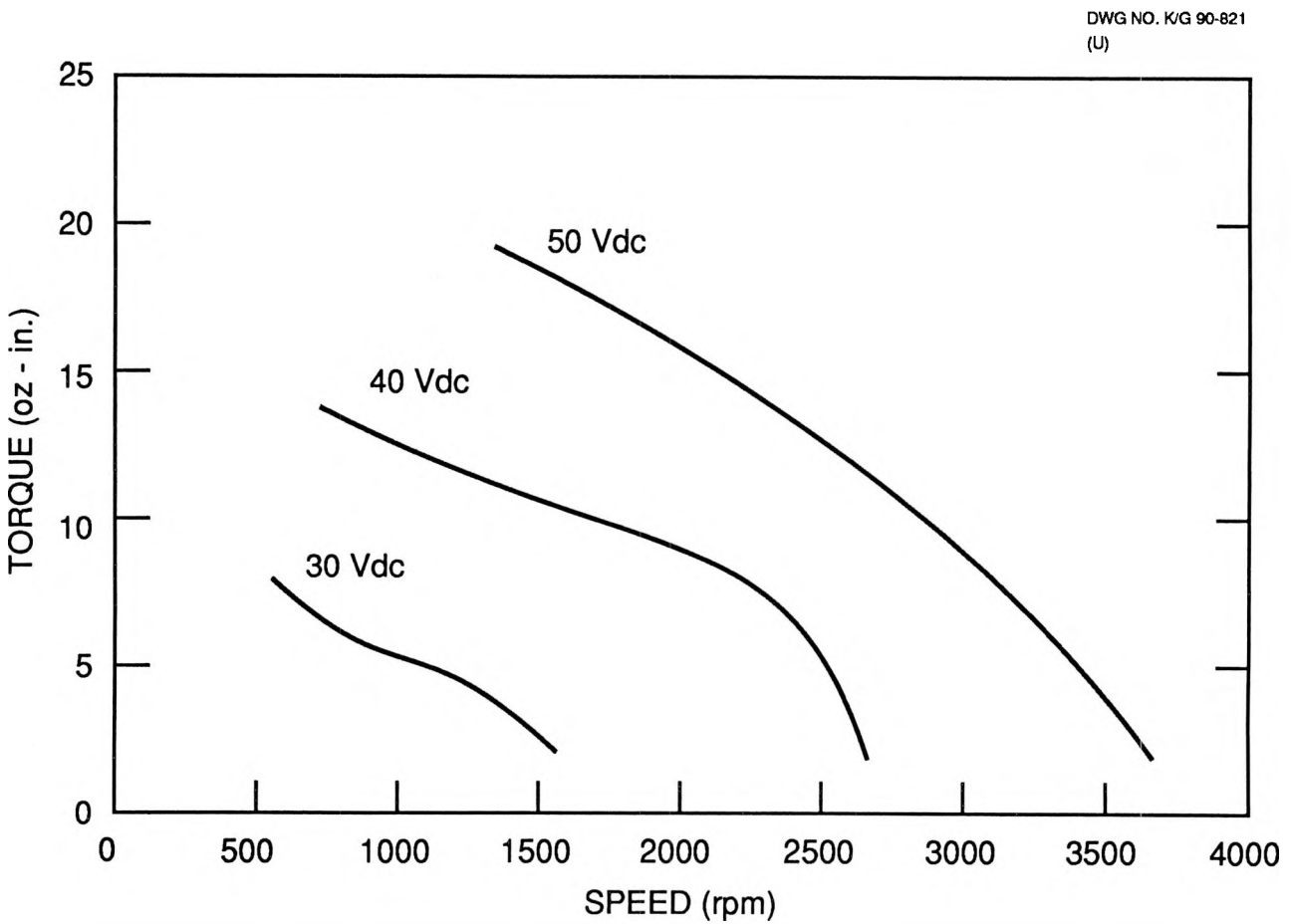

Fig. 8. Torque vs speed for 0.250-in. air gap and dry bearing using half-bridge drive system.

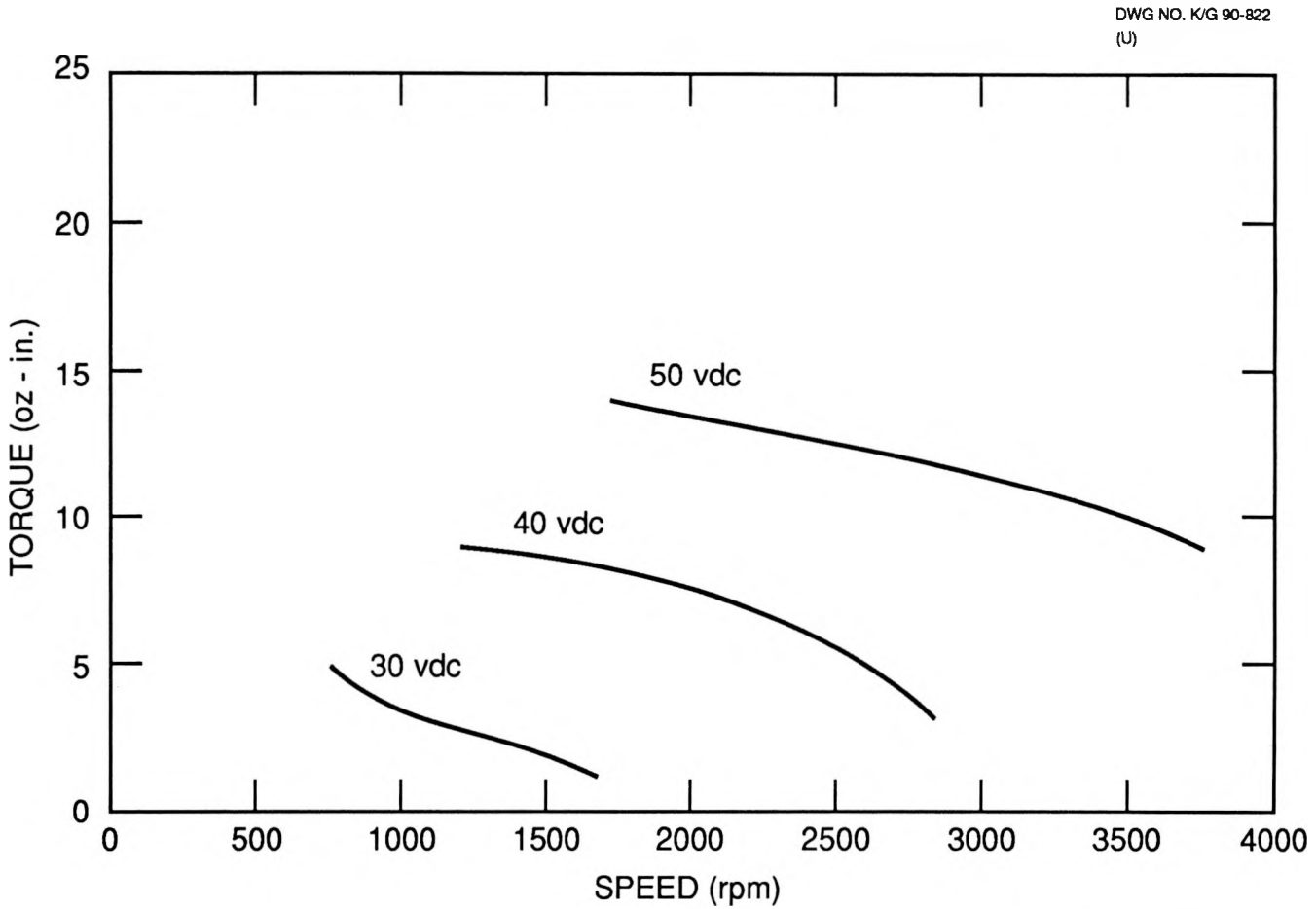

Fig. 9. Torque vs speed for 0.300-in. air gap and dry-bearing using half-bridge drive system.

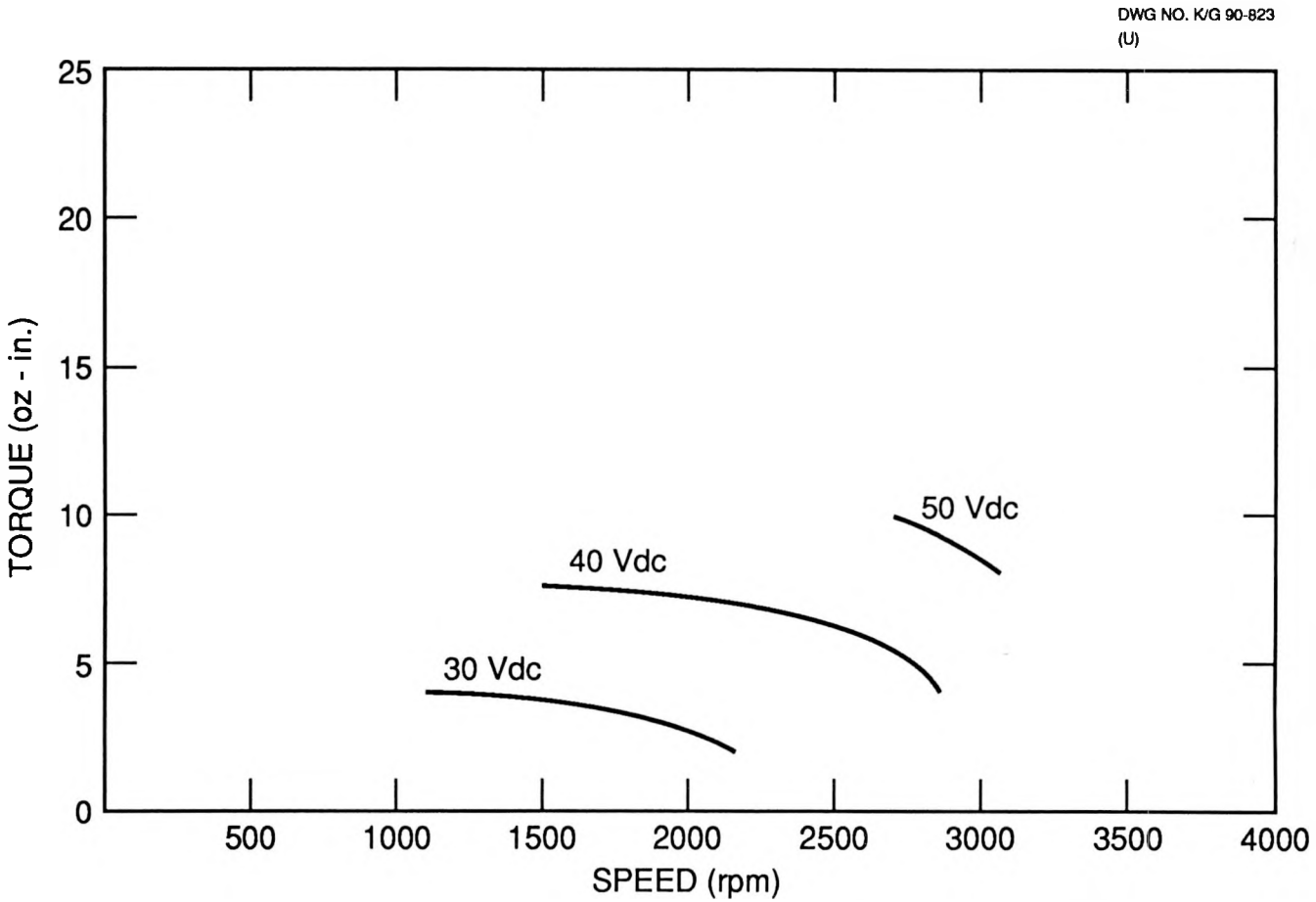

Fig. 10. Torque vs speed for 0.350-in. air gap and dry bearing using half-bridge drive system.

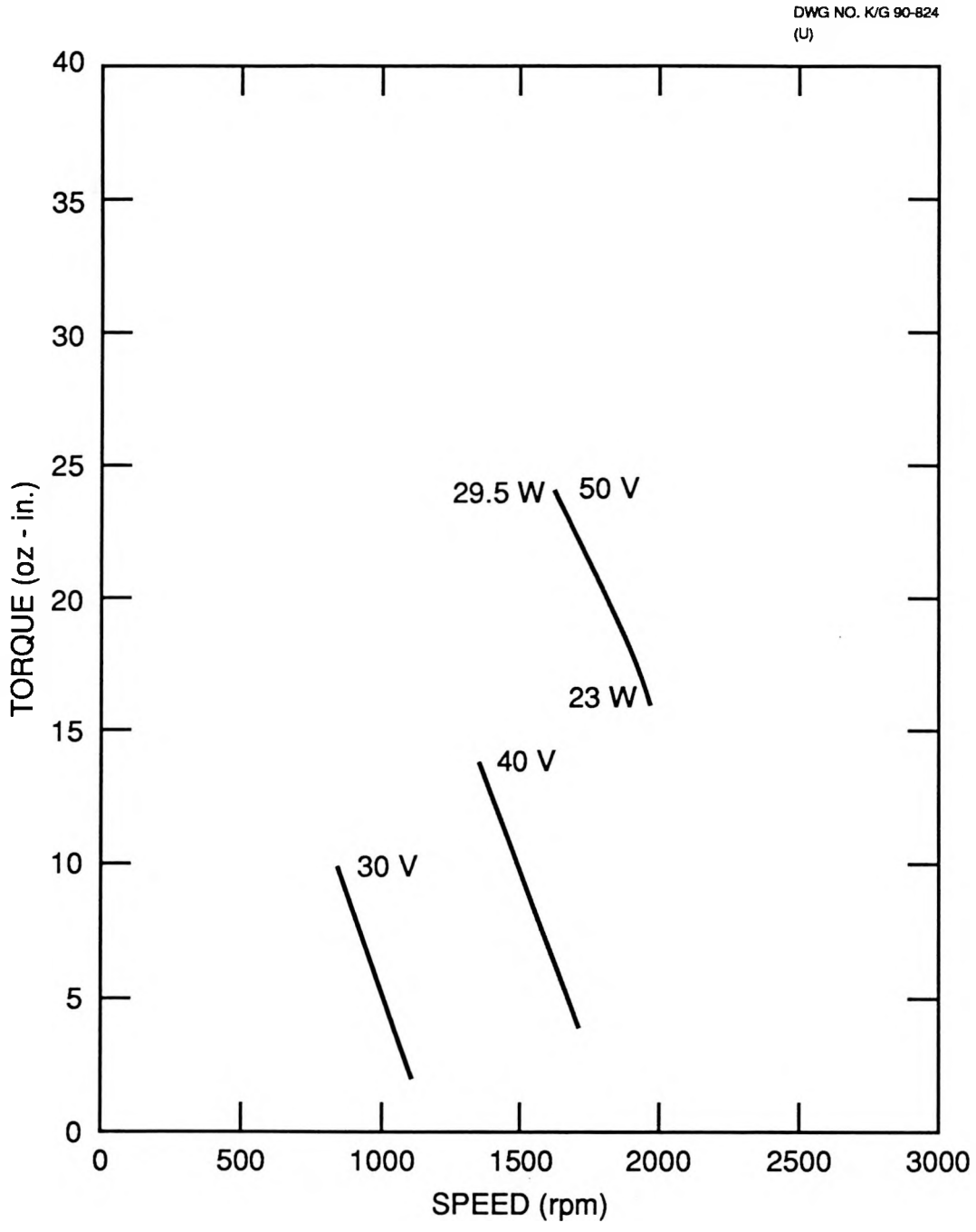

Fig. 11. Torque vs speed for 0.050-in. air gap and water-lubricated bearing.

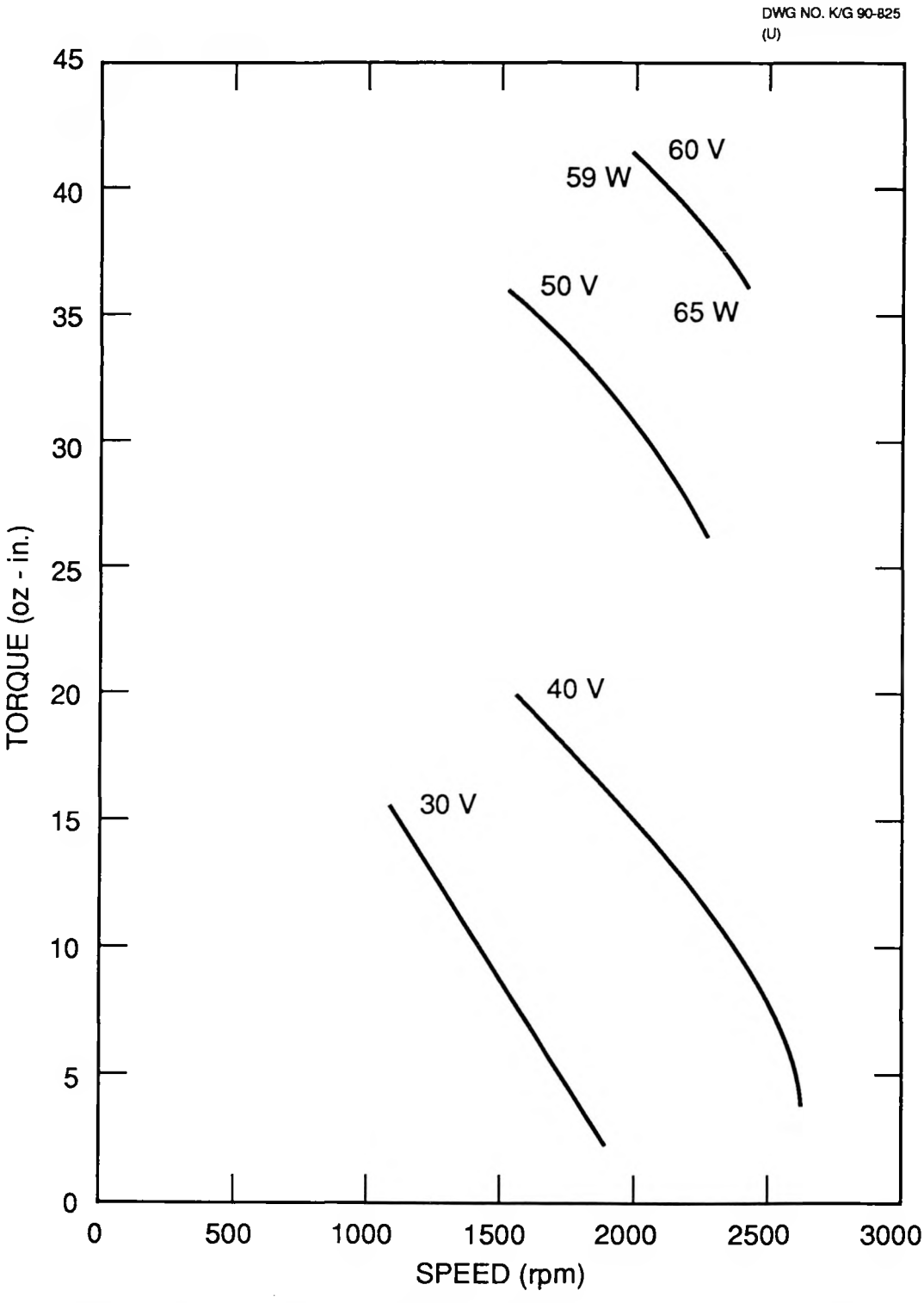

Fig. 12. Torque vs speed for 0.150-in. air gap and water-lubricated bearing.

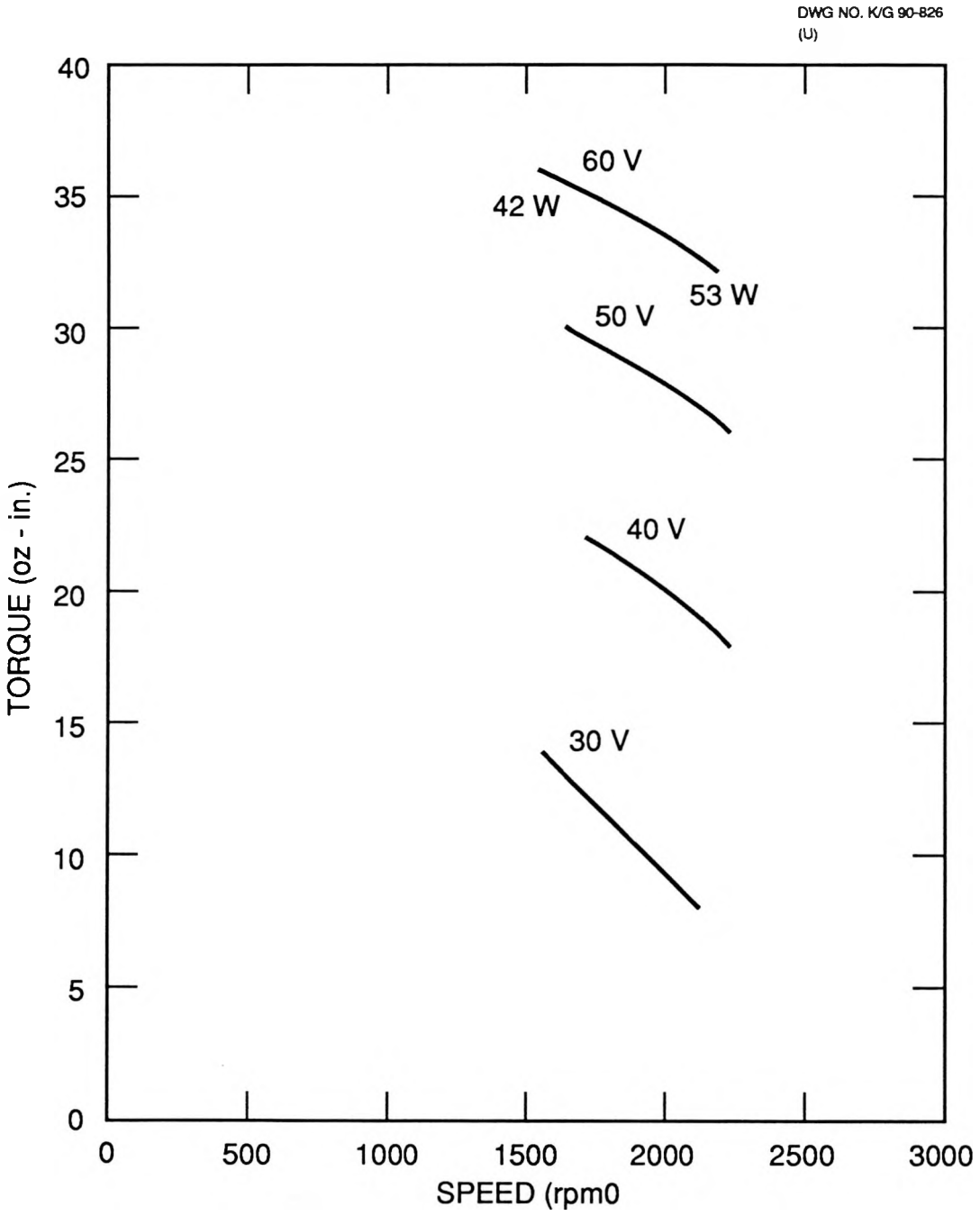

Fig. 13. Torque vs speed for 0.250-in. air gap and water-lubricated bearing.

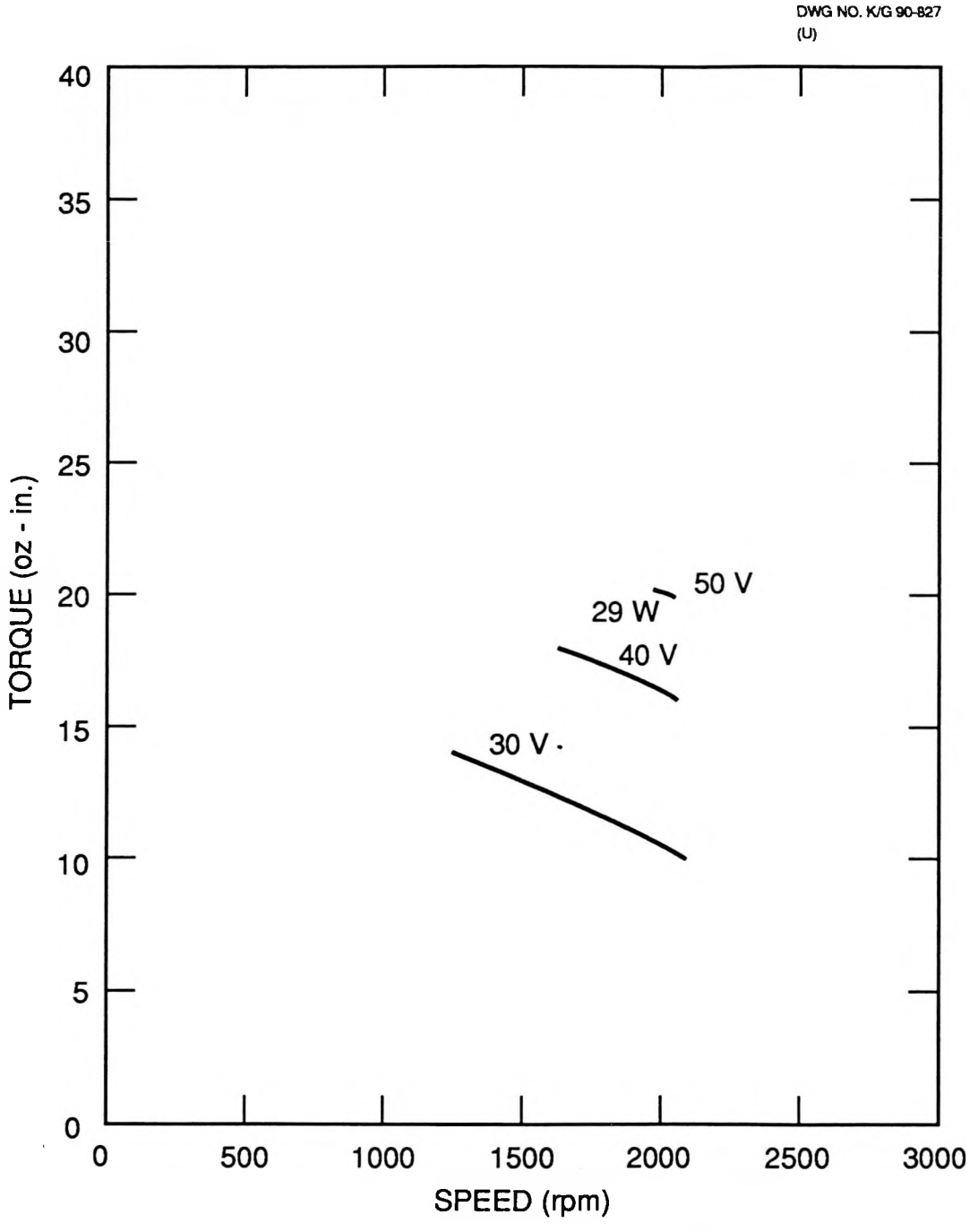

Fig. 14. Torque vs speed for 0.350-in. air gap and water-lubricated bearing.

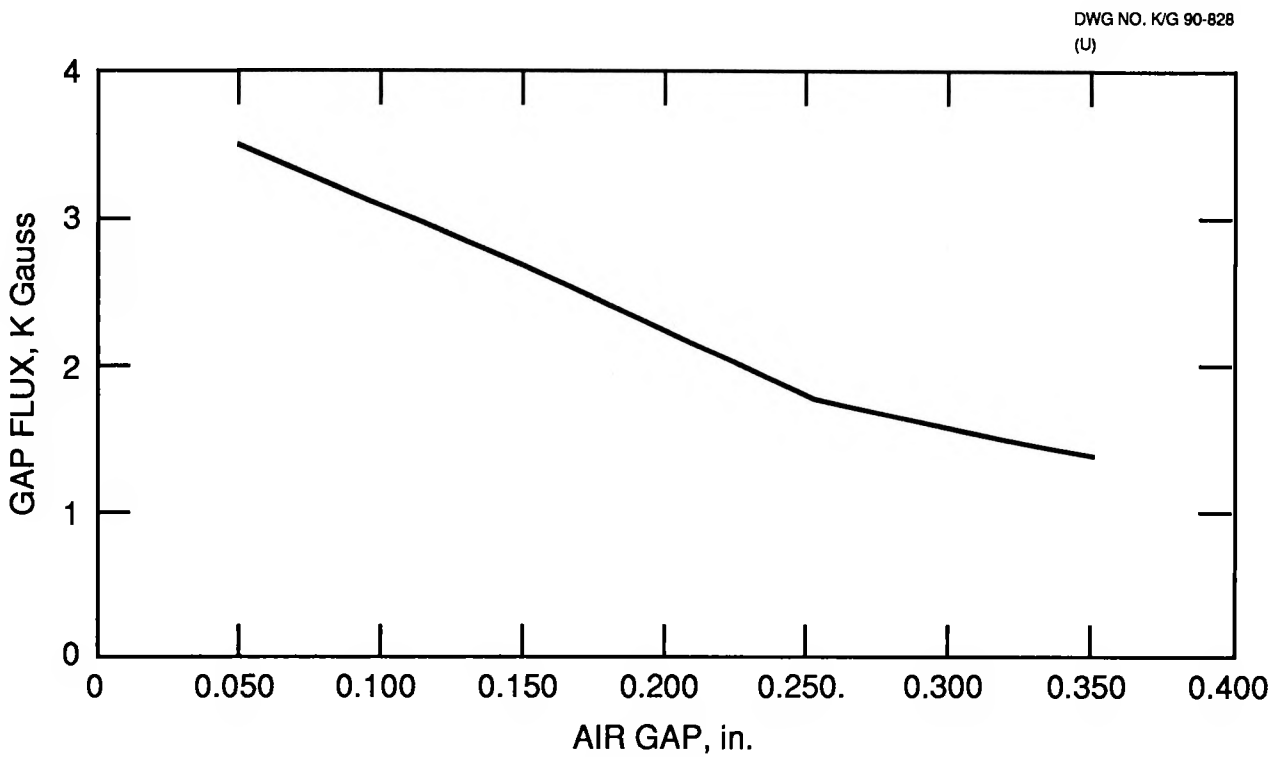

Fig. 15. Air-gap flux density vs distance.

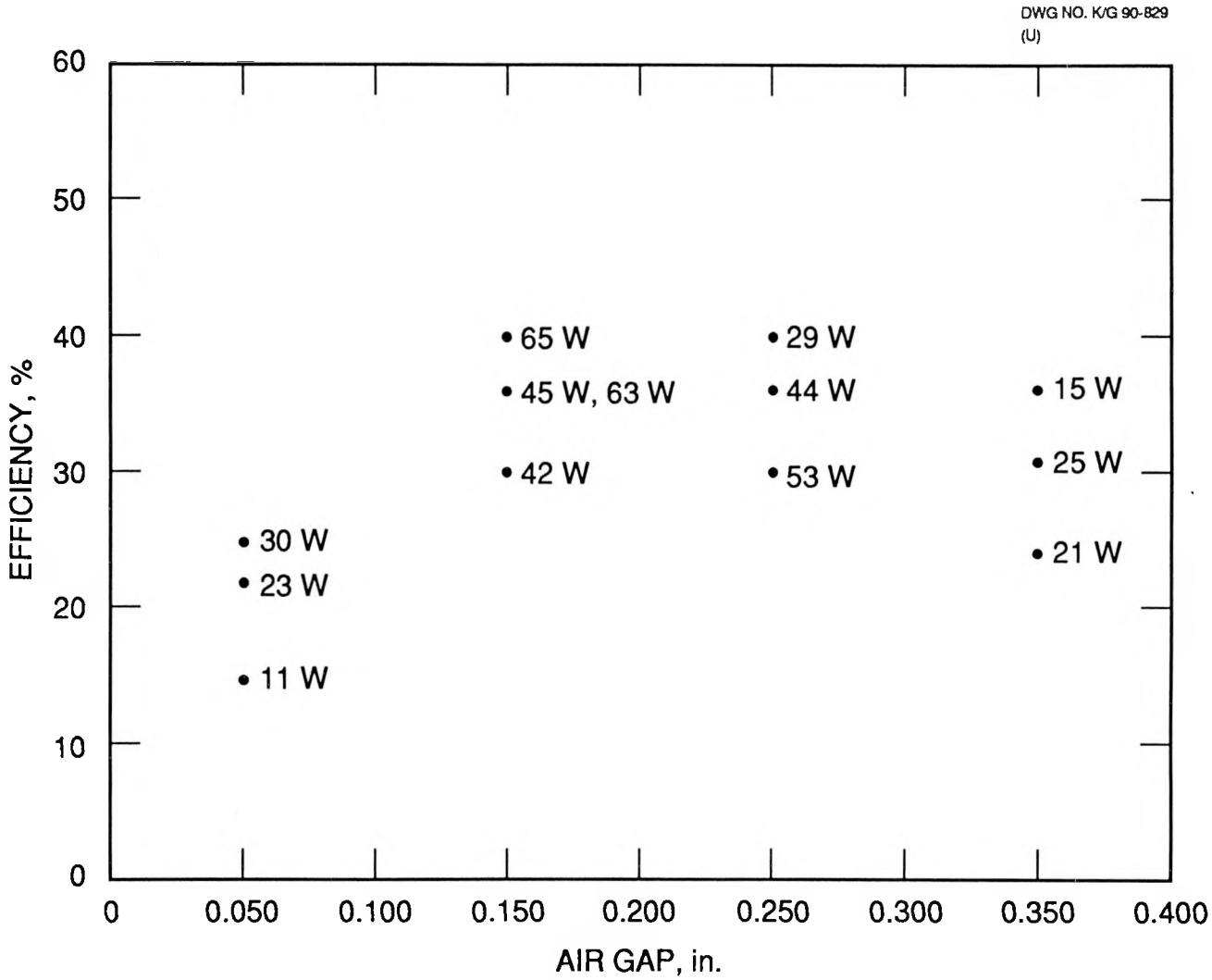

Fig. 16. Efficiency of water-lubricated bearing and motor system vs air-gap distance using half-bridge drive.

Internal Distribution

1. D. S. Daniel
2. R. C. Devault
3. P. D. Fairchild
4-5. R. A. Hawsey
6. L. G. Horner
7. J. G. Hubrig
8-11. P. J. Hughes
12. W. S. Key
13. C. W. Sohns
14. Applied Technology Library
15. Central Research Library
16. Y-12 Technical Library
17. ORNL Patent Section
18-19. Laboratory Records Department
20. Laboratory Records - RC

External Distribution

21. Dr. J. M. Bailey, Department of Electrical and Computer Engineering, 320 Ferris Hall, The University of Tennessee, Knoxville, Tennessee 37996-2100.